

Emitting modification in Si-rich-SiN_x films versus silicon nitride compositions

T. Torchynska, Instituto Politécnico Nacional, ESFM, México DF, 07738, México

G. Polupan, Instituto Politécnico Nacional, ESIME, México DF, 07320, México

L. Khomenkova, V. Lashkaryov Institute of Semiconductor Physics at NASU, Kyiv, 03028, Ukraine

A. Siaoui, ICube, 23 rue du Loess, BP 20 CR, 67037 Strasbourg Cedex 2, France

Address all correspondence T. Torchynska, L. Khomenkova at torch@esfm.ipn.mx; khomen@ukr.net

(Received 27 April 2017; accepted 31 May 2017)

Abstract

SiN_x films were grown by plasma-enhanced chemical vapor deposition on Si substrates with the composition controlled by the flow ratio R : ammonia to silane in the range $R = 0.45$ – 1.0 . Then SiN_x films were annealed at 1100 °C for 30 min to form Si-quantum dots (QDs). Fourier transform infrared spectroscopy study permits estimating SiN_x compositions. Photoluminescence (PL) spectra of SiN_x films included bands peaked at: 2.87–2.99, 2.42–2.54, 2.10–2.25, and 1.47–1.90 eV. Former three PL bands are attributed to emission via defects in SiN_x films. Fourth PL band is assigned to exciton emission in Si QDs, detected by transmission electron microscopy study in films grown at $R \leq 0.67$. The nature of non-radiative defects in SiN_x films is discussed as well.

Introduction

Silicon nitride (Si₃N₄)-based materials have been extensively investigated in the last decades owing to their interesting chemical, mechanical, and optical properties.^[1] The creation of Si-quantum dots (QDs) in a SiN_x host offers the several key advantages over Si oxide.^[2] Silicon nitride is a more promising matrix for Si-QDs due to its structural stability at electronic technology processing. Better electrical properties owing to the lower tunneling barrier allow the transport of electrons and holes into Si-QDs embedded in SiN_x.^[3] Additionally, the Si-QDs coordinated with oxygen atoms are subject to charge trapping at the interface states, which limit the energy of emission quantas from Si-QDs to <2 eV.^[4] Since Si-QDs coordinated with nitrogen (N) atoms do not exhibit this limitation, the photoluminescence (PL) is expected to occur at energies across the wide visible spectral range.^[3,5,6]

Si-QD formation in SiN_x is also more favorable owing to the lower annealing temperature required in comparison with Si oxide.^[7,8] The Si-QD formation in SiN_x films has been found to occur as a complex process, with the appearance of amorphous and crystalline clusters and a strong dependence on deposition and processing conditions.^[3,9,10]

In majority reports,^[5,6,9] PL was ascribed to the quantum confinement effects in Si-QDs. However, other authors^[11–13] considered the radiative transitions via defects in SiN_x. The variation of PL peaks with QD sizes is a basis to attribute the PL bands to the exciton recombination in Si-QDs. However, in a set of cases the different PL peaks were assigned to the Si-QDs of the same sizes in SiN_x. This fact indicates that PL

bands connected with the recombination of excitons in Si-QDs or carriers via SiN_x defects were not discriminated clearly yet.

In this work, the luminescent properties of Si-rich-SiN_x films grown by plasma-enhanced chemical vapor deposition (PECVD) were investigated versus excess Si content in the temperature range 10–300 K. The detailed analysis of the results allows getting insight in the nature of emission and non-radiative processes in the SiN_x films.

Experimental details

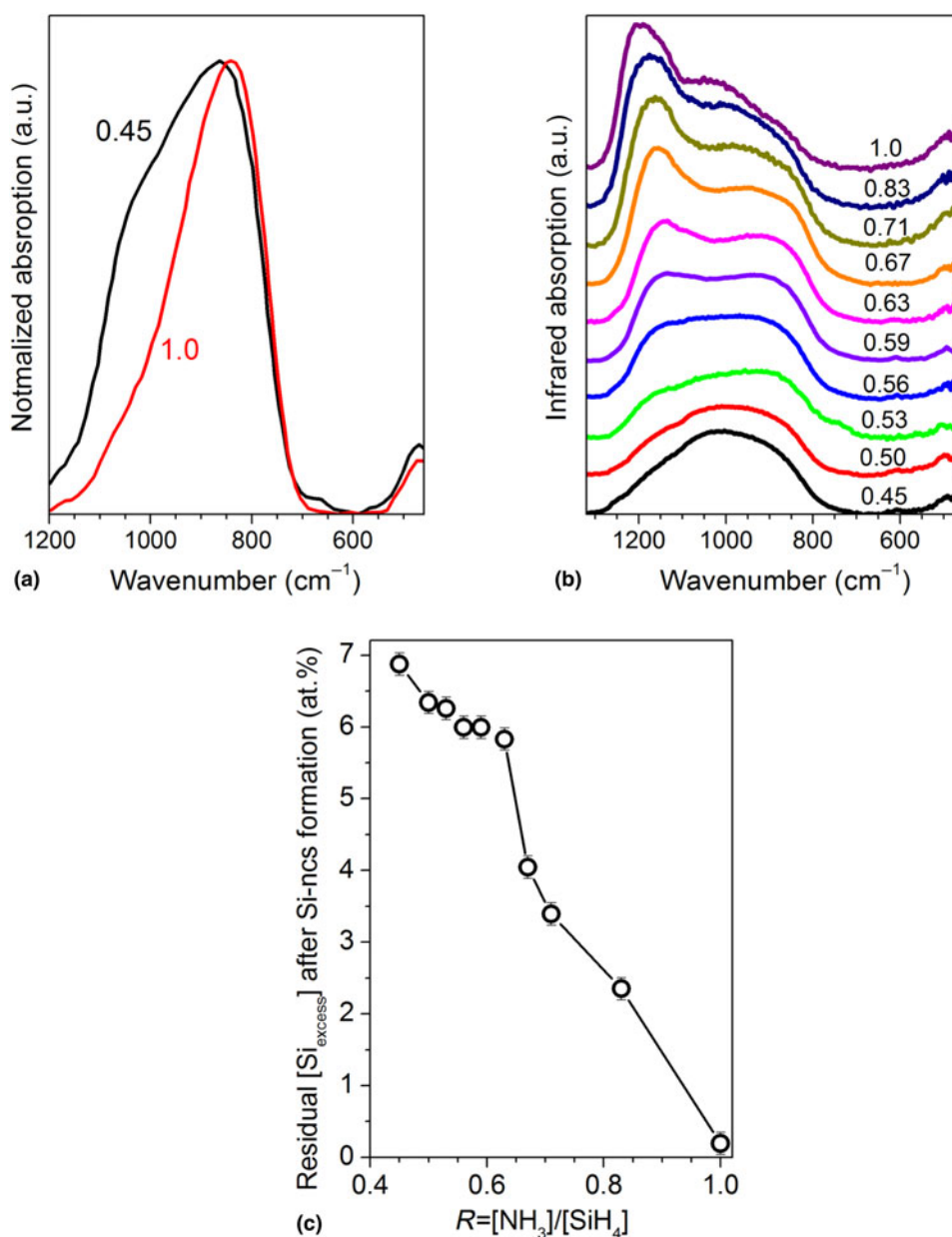
Si-rich SiN_x films were grown by PECVD on p-type Si (001) substrates. To achieve different stoichiometry, the NH₃/SiH₄ gas flow ratio (R) was varied in the range of $R = 0.45$ – 1.0 keeping SiH₄ flow constant at 14 sccm (Table I). The working pressure, plasma power, and growth temperature were 0.5 Torr, 20 W, and 350 °C, respectively. Thermal annealing at 1100 °C for 30 min in N flow was applied to produce the Si-QDs in the SiN_x films.^[13]

Fourier transform infrared spectroscopy (FTIR) was recorded in the range of 460–4000 cm⁻¹ using a Nicolet Nexus spectrometer under normal and Brewster angle (65°) configurations. PL spectra were excited by 325-nm line of a He–Cd laser with a beam power 76 mW. More details about PL experiments can be found elsewhere.^[14,15] To investigate the evolution of PL with temperature in the range of 10–300 K, the films were mounted in a closed-cycle He cryostat.

To confirm the formation of Si-QDs the samples were prepared for transmission electron microscopy (TEM) observations

Table I. Technological parameters of SiN_x films.

Parameters	Sample numbers									
	#1	#2	#3	#4	#5	#6	#7	#8	#9	#10
NH ₃ flow (sccm) at SiH ₄ flow = 14.0 sccm	14.0	11.6	10.0	9.5	8.8	8.2	7.8	7.4	7.0	6.3
Gas ratio $R = [\text{NH}_3]/[\text{SiH}_4]$	1.00	0.83	0.71	0.67	0.63	0.59	0.56	0.53	0.50	0.45
x in as-deposited SiN _{x}	0.82	0.61	0.50	0.46	0.42	0.39	0.37	0.34	0.30	0.28

**Figure 1.** (a) Normal-incidence FTIR spectra obtained for as-deposited SiN_x films with $R = 0.45$ and 1.0 . (b) Brewster-incidence FTIR spectra of films annealed at $1100\text{ }^\circ\text{C}$ for 30 min. (c) Estimated residual Si excess in annealed films after the Si-QD formation.

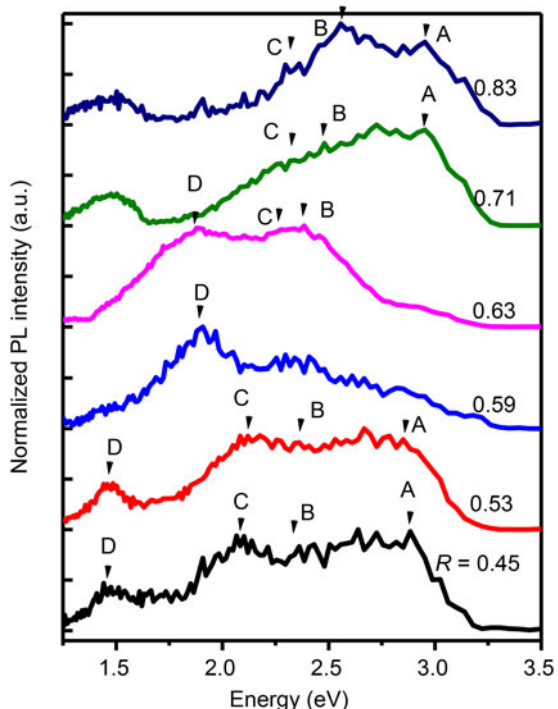


Figure 2. PL spectra of annealed films versus R measured at 3.82 eV excitation light energy. The spectra were normalized on the intensity of their maximum.

by the standard procedure involving grinding, dimpling, and Ar^+ ion beam thinning until electron transparency. Then the samples were studied by high resolution TEM (HR-TEM) on a JEOL 2100F operating at 200 keV and equipped with a corrector for spherical aberration and with the last generation of Gatan imaging filters.^[16]

Results and discussion

The microstructure of studied films was investigated by the FTIR method. The most efficient vibration bands in hydrogenated SiN_x films are observed for Si–N ($470\text{--}490$, $830\text{--}870$, and $1190\text{--}1200\text{ cm}^{-1}$), Si–H ($650\text{--}660$ and $2250\text{--}2300\text{ cm}^{-1}$) and N–H ($1180\text{--}1200$ and $3340\text{--}3380\text{ cm}^{-1}$) vibration modes.^[9,17] FTIR spectra of SiN_x films detected with a normal incidence show significant overlapping of Si–N vibration bands and only one broad band in the range of $600\text{--}1200\text{ cm}^{-1}$ can be seen [Fig. 1(a)]. At the same time, the spectra recorded with a Brewster incidence angle ($\sim 65^\circ$) as a rule shows well-separated Si–N bands at about 1140 and 930 cm^{-1} , ascribed respectively to the longitudinal (LO) and transverse (TO) modes of the Si–N stretching vibration.^[9,17]

FTIR spectra of all studied as-deposited films demonstrate the broad bands with the maxima at $830\text{--}880$ and $460\text{--}480\text{ cm}^{-1}$ [Fig. 1(a)], which are attributed to the Si–N symmetric and asymmetric stretching vibrations, respectively.^[9,17] The peak position of the Si–N stretching band depends on the R value demonstrating the shift to higher wavenumbers with R decreasing [Fig. 1(a)]. Such behavior can be explained by increasing the Si content in the plasma, when Si atoms have not enough N atoms to form the Si–N bonds. This will cause film disordering and broadening the FTIR bands.^[17] In contrary, the shift of peaks from 945.3 to 848.6 cm^{-1} is accompanied by band narrowing due to improving the SiN_x film quality.^[18] In our case, R decreasing results in the higher disorder of SiN_x films due to increasing the Si excess content. Besides, N content lowering in plasma will stimulate more prominent incorporation of hydrogen in the films.^[13] This is evident as well by appearing a shoulder at about $650\text{--}660\text{ cm}^{-1}$ [Fig. 1(a)] that is related to the Si–H vibration modes.^[9,17]

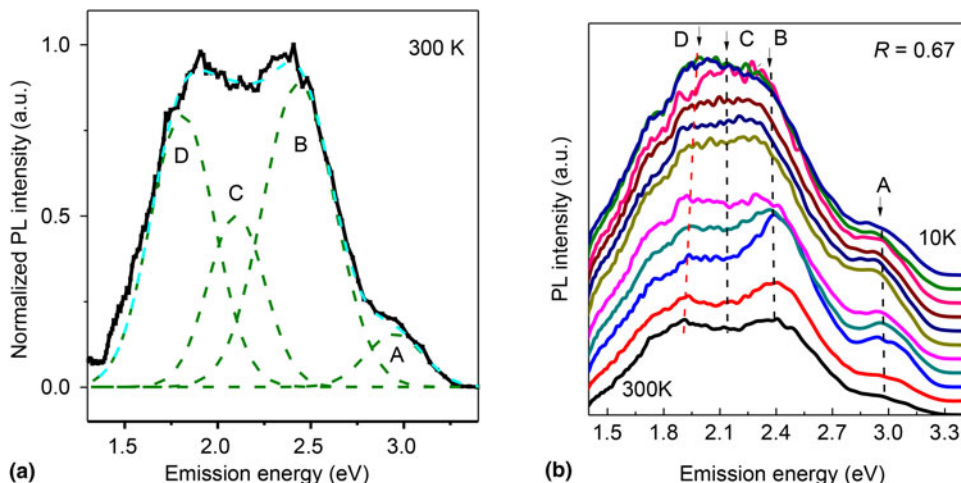


Figure 3. Deconvolution of PL spectrum (a) excited by the light with energy 3.82 eV and measured at 300 K for the film grown with $R=0.67$. PL spectra (b) of the film obtained at $R=0.67$ and measured in the range 10–300 K.

High-temperature annealing results in a transformation of FTIR spectra. Si–H related bands, as a rule, vanish due to hydrogen out-diffusion from the films. Simultaneously, the broken Si and N dangling bonds will try to saturate each other via the formation of Si–N and Si–Si bonds related to the Si phase [Fig. 1(b)]. Si–N peak increasing at $1180\text{--}1200\text{ cm}^{-1}$ demonstrates the formation of the Si/SiN_x interface that is more prominent for films grown at higher R values [Fig. 1(b)]. However, the Si–N peak position at 900 cm^{-1} testifies on significant disordering in the films obtained at small R values that can be due to the presence of crystalline Si-QDs and amorphous Si phases (Fig. 1(b)).

The Si–N band position is well described by a model based on linear combination of weighted bonding density^[17] that allows determining the film stoichiometry x (Table I) using the formula:

$$\nu_{\text{LO}} = 323.4 \times (x - 0.75) + 1197. \quad (1)$$

This formula is based on the comparison of LO peak variation in studied films with its position in Si₃N₄ ($\sim 1197\text{ cm}^{-1}$). Additionally, the comparison of LO peak positions in as-deposited and annealed films allows estimating the residual Si excess in films after the Si-QD formation. In the films grown with $R > 0.8$, almost all excess Si atoms have been coagulated into Si-QDs. But the SiN_x films fabricated with lower R still demonstrate the presence of excess Si [Fig. 1(c)].

Room-temperature PL spectra of annealed samples demonstrate the variation of their shape versus film compositions (Fig. 2). With R decreasing the PL spectra demonstrate the appearance of asymmetry in the low-energy side (Fig. 2). The total PL peak position has shifted toward the lower energies, but it does not demonstrate a systematic shift with R (Fig. 2).

The analysis of PL spectra has revealed that all PL spectra can be decomposed (Fig. 3) on four PL bands with the maxima at: 2.87–2.99 eV (A), 2.42–2.54 eV (B), 2.10–2.25 eV (C), and 1.47–1.90 eV (D) in different samples. It is clear that PL peaks

A, B, and C dominate in PL spectra of films grown at $R = 0.71\text{--}1.0$ (Fig. 2). The PL peaks A, B, and C shift at nearly 120 meV: from 2.99, 2.54, 2.25 eV down to 2.87, 2.42, 2.13 eV, respectively, with R decreasing (Fig. 2).

In SiN_x films grown at $R = 0.59\text{--}0.67$, the PL band peaked at 1.90 eV (D) appears and dominates in PL spectra at 300 K (Fig. 2). Its peak shifts to 1.47 eV (Fig. 2) with increasing the Si content in the films when R decreases to 0.45. The spectral shift of D-band peak is more significant (430 meV) than the shifts of other PL bands A, B, and C related to changing the SiN_x film compositions.

The evolution of integrated PL intensities for the PL bands A, B, C, and D versus R is presented in Fig. 4(a). PL intensities increase when R decreases from 1.0 to 0.71; approach the highest values for $R = 0.59\text{--}0.67$ and decrease for $R \leq 0.59$ [Fig. 4(a)]. Figure 4(b) represents varying the optical band gap of SiN_x films versus R obtained from published early papers (Refs 19–22). This figure shows that the quantum energy of excitation light used (3.82 eV) becomes equal or exceeds the optical band gap in films grown at $R \leq 0.67$ that explains the highest PL intensity observed for the films grown at $R = 0.59\text{--}0.67$ [Fig. 4(a)]. It is clear that our experimental results are in the agreement with those presented in Refs 19, 20. Simultaneously, the possibility to detect the A- and B-PL bands in PL spectra of the films grown at $R = 0.45\text{--}0.53$ testifies on the large optical band gap ($\sim 3.0\text{ eV}$) in these films being similar to the data of Ref. 19.

Based on the models proposed early in Refs 23–25, the 2.87–2.99 eV (A) and 2.42–2.54 eV (B) PL bands can be ascribed to the native defects in SiN_x, such as the N dangling bonds (N₄⁺ and N₂⁰, $\sim 3.0\text{ eV}$) and the Si dangling bonds (called K⁰-centers, $\sim 2.40\text{--}2.50\text{ eV}$), respectively. The PL band at 590 nm (2.1 eV) was assigned early to oxygen related defects in SiN_x.^[26] Another interpretation for the PL band 2.10–2.25 eV (C) was proposed in Ref. 23, where this band was attributed to the carrier recombination between N₄⁺ and N₂⁰ energy levels in SiN_x.

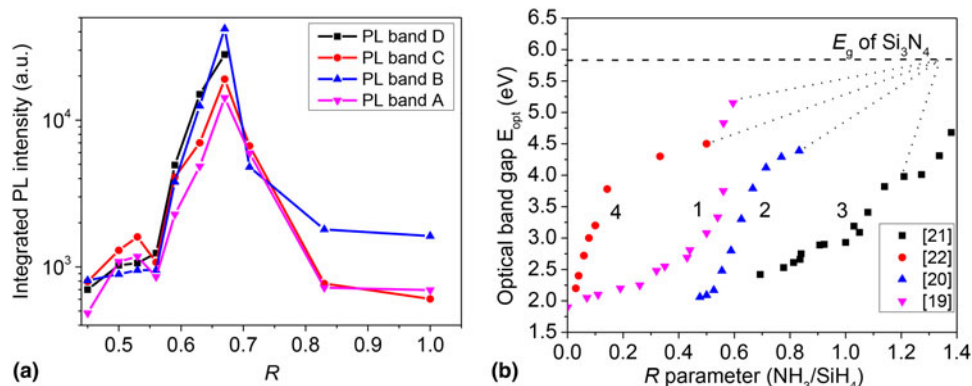


Figure 4. The variations of integrated PL intensities (a) for different PL bands versus R . The variation of optical band gap (b) in SiN_x films versus R were taken from Refs: 1- [19], 2- [20], 3- [21], and 4- [22].

The PL band D demonstrates the shift of PL peaks from 1.90 to 1.47 eV with increasing the excess Si content and this shift (430 meV) is more significant than the shifts (120 meV) of other PL bands (Fig. 2). The last fact permits to assign the PL band D to exciton recombination inside of Si-QDs of different sizes. The size of Si-QDs can be estimated from the D peak positions using formula $E = 1.13 + 13.9/d^2$, proposed in Ref. 27. This estimation gives the Si-QD sizes from 3.5 nm up to 6.2 nm for varying the PL peak D from 1.90 to 1.47 eV, respectively. In case of a film grown with $R = 0.63$, the presence of Si-QDs with the size of 3.5–4.0 nm has been demonstrated by the bright-field HR-TEM.^[11]

To gain insight on light-emitting mechanisms in SiN_x films, PL measurements within the range of 10–300 K have been performed [Fig. 3(b)]. This investigation has revealed that the PL band D demonstrates the shift of PL peaks with heating (50 meV) similar to the shrinkage of the Si band gap. The D peak at 10 K was found to be 1.95 eV and it shifts to 1.90 eV at 300 K. Simultaneously, the other PL peaks A, B, and C do not change their peak positions with heating [Fig. 3(b)]. Taking into account the spectral position of the PL band D and its behavior at the variation of temperatures and Si excess contents, one can conclude that this PL band D is due to the exciton recombination inside of Si-QDs.^[28]

Integrated PL intensities of all PL bands decrease dramatically in films obtained at small $R \leq 0.56$ [Fig. 4(a)] that can be owing to the enhanced non-radiative recombination, which is connected with the high residual amorphous Si content [Fig. 1(c)]. Additionally, it is clear that the PL intensity of D-band decreases faster versus R in comparison with intensities of others PL bands (Fig. 2). This fact can be related to the size enlargement of crystalline Si-QDs with increasing Si content that is accompanied by quenching the exciton emission efficiency inside of Si-QDs.^[29]

Conclusions

Si-rich – SiN_x films were fabricated by PECVD on the Si substrates. The PL spectrum investigation of SiN_x films with different compositions gives the possibility to extract the information concerning different radiative channels in SiN_x emission. The main contribution in PL spectra is given by the carrier recombination via native defects in SiN_x films fabricated at $R \geq 0.63$. In films obtained at $R = 0.59–0.67$, the exciton recombination inside of Si-QDs form the dominated radiative channel. The efficient non-radiative recombination was revealed in the films obtained at $R \leq 0.56$ and attributed to the residual amorphous Si content in SiN_x. The high PL intensity is determined in SiN_x films obtained at $R = 0.59–0.67$.

Supplementary material

The supplementary material for this article can be found at <https://doi.org/10.1557/mrc.2017.39>.

Acknowledgments

The author T. T. thanks the SIP-IPN (project 20170821) and CONACYT, Mexico (project 258224), as well as L. K. thanks the National Academy of Sciences of Ukraine for the financial supports.

References

- V.I. Belyi, L.L. Vasilyeva, R. Gennann, A.S. Ginovker, V.A. Gritsenko, S.M. Repinsky, S.P. Sinitza, T.P. Smirnova, and F.L. Edelman. In *Silicon Nitride in Electronics, Materials Science Monographs*, edited by V.I. Belyi (Elsevier Science Ltd, Amsterdam, 1988), vol. 34.
- L. Pavesi and D.J. Lockwood, *Silicon Photonics* (Springer-Verlag, Berlin, 2004), 398 p.
- G.Y. Sung, N.M. Park, J.H. Shin, K.H. Kim, T.Y. Kim, K.S. Cho, and C. Huh: Physics and device structures of highly efficient silicon quantum dots based silicon nitride light-emitting diodes. *IEEE J. Sel. Top. Quantum Electron.* **12**, 1545 (2006).
- M. Wolkov, J. Jorne, P. Fauchet, G. Allan, and C. Delerue: Electronic states and luminescence in porous silicon quantum dots: the role of oxygen. *Phys. Rev. Lett.* **82**, 197 (1999).
- N.M. Park, C.J. Choi, T.Y. Seong, and S.J. Park: Quantum confinement in amorphous silicon quantum dots embedded in silicon nitride. *Phys. Rev. Lett.* **86**, 1355 (2001).
- L. Dal Negro, J.H. Yi, V. Nguyen, Y. Yi, J. Michel, and L.C. Kimerling: Spectrally enhanced light emission from aperiodic photonic structures. *Appl. Phys. Lett.* **86**, 261905 (2005).
- D. Comedi, O.H.Y. Zalloum, J. Wojcik, and P. Mascher: Light emission from hydrogenated and unhydrogenated Si-nanocrystal/Si dioxide composites based on PECVD-grown Si-rich Si oxide films. *IEEE J. Sel. Top. Quantum Electron.* **12**, 1561 (2006).
- R. Pratibha Nalini, L. Khomenkova, O. Debieu, J. Cardin, C. Dufour, M. Carrada, and F. Gourbilleau: SiO_x/SiN_y multilayers for photovoltaic and photonic applications. *Nanoscale Res. Lett.* **7**, 124 (2012).
- F. Delachat, M. Carrada, G. Ferblantier, and A. Slaoui: Properties of silicon nanoparticles embedded in SiN_x deposited by microwave-PECVD. *Nanotechnology* **20**, 415608 (2009).
- A.-S. Keita, A. En Naciri, F. Delachat, M. Carrada, G. Ferblantier, and A. Slaoui: Spectroscopic ellipsometry investigation of the optical properties of nanostructured Si/SiN_x films. *J. Appl. Phys.* **107**, 093516 (2010).
- T.V. Torchynska, J.L. Casas Espinola, E. Vergara Hernandez, L. Khomenkova, F. Delachat, and A. Slaoui: Effect of the stoichiometry of Si-rich silicon nitride thin films on their photoluminescence and structural properties. *Thin Solid Films* **581**, 65 (2015).
- T.V. Torchynska, J.L. Casas Espinola, L. Khomenkova, E. Vergara Hernandez, J.A. Andraca Adame, and A. Slaoui: Structural and light emitting properties of silicon-rich silicon nitride films grown by plasma enhanced-chemical vapor deposition. *Mater. Sci. Semicond. Proc.* **37**, 46 (2015).
- F. Delachat, Elaboration and characterization of Si-licon nanoparticles in silicon nitride for photovoltaic application, Ph.D. Thesis, ESS-University of Strasbourg, France, 2010.
- T.V. Torchynska, Y. Goldstein, A. Many, J. Jedrzejewskii, and A. V. Kolobov: Mechanism of photoluminescence of silicon oxide films enriched by Si or Ge. *Microelectron. Eng.* **66**, 83 (2003).
- L. Khomenkova, F. Gourbilleau, J. Cardin, O. Jambois, B. Garrido, and R. Rizk: Long lifetime and efficient emission from Er³⁺ ions coupled to Si nanoclusters in Si-rich SiO₂ layers. *J. Lumin.* **129**, 1519 (2009).
- G. Scardera, T. Puzzer, I. Perez-Wurfl, and G. Conibeer: The effects of annealing temperature on the photoluminescence from silicon nitride multilayer structures. *J. Cryst. Growth* **310**, 3680 (2008).
- D.V. Tsu, G. Lucovsky, and M.J. Mantini: Local atomic structure in thin films of silicon nitride and silicon diimide produced by remote plasma-enhanced chemical-vapor deposition. *Phys. Rev. B* **33**, 7069 (1986).
- V.K. Tomar, L.S. Patil, and D.K. Guatam: Deposition and characterization of silicon nitride films using HMDS for photonics applications. *J. Optoelectron. Adv. Mater.* **10**, 2657 (2008).

19. H.S. Nalwa, *Silicon-Based Materials and Devices: Properties and Devices* (Academic Press, 2001), vol. **1**, Chapter 5, pp. 210–211.
20. H.L. Hsiao, A.B. Yang, and H.L. Hwang: Luminescence and structural properties of silicon-rich nitride by X-ray absorption spectroscopy. *J. Phys. Chem. Solids* **69**, 278 (2008).
21. L.V. Goncharova, P.H. Nguyen, V.L. Karner, R. D'Ortenzio, S. Chaudhary, C.R. Mokry, and P.J. Simpson: Si quantum dots in silicon nitride: quantum confinement and defects. *J. Appl. Phys.* **118**, 224302 (2015).
22. J. Kistner, X. Chen, Y. Weng, H.P. Strunk, M.B. Schubert, and J. H. Werner: Photoluminescence from silicon nanocrystals embedded in silicon nitride fabricated by low-pressure chemical vapor deposition followed by high-temperature annealing. *J. Appl. Phys.* **110**, 023520 (2011).
23. S.V. Deshpande, E. Gulari, S.W. Brown, and S.C. Rand: Optical properties of silicon nitride films deposited by hot filament chemical vapor deposition. *J. Appl. Phys.* **77**, 6534 (1995).
24. C.M. Mo, L.D. Zhang, C.Y. Xie, and T. Wang: Luminescence of nanometer-sized amorphous silicon nitride solids. *J. Appl. Phys.* **73**, 5185 (1993).
25. W.I. Warren, P.M. Lenahan, and S.E. Curry: First observation of paramagnetic nitrogen dangling-bond centers in silicon nitride. *Phys. Rev. Lett.* **65**, 207 (1990).
26. B. Sain, and D. Das: Tunable photoluminescence from nc-Si/a-SiN_x:H quantum dot thin films prepared by ICP-CVD. *Phys. Chem. Chem. Phys.* **15**, 3881 (2013).
27. C.H. Cho, B.H. Kim, N.M. Park, and G.Y. Sung: Effect of hydrogen passivation on charge storage in silicon quantum dots embedded in silicon nitride film. *Appl. Phys. Lett.* **86**, 143107 (2005).
28. T.V. Torchynska, Nanocrystals and quantum dots. Some physical aspects. In *Nanocrystals and Quantum Dots of Group IV Semiconductors*, edited by T.V. Torchynska, Yu. Vorobiev (American Scientific Publisher, Stevenson Ranch, CA, USA) 2010, p.1–40.
29. T.V. Torchynska: Quantum emission efficiency of nanocrystalline and amorphous Si quantum dots. *Physica E* **44**, 56 (2011).